

Oxidation Catalysts Based on Tin-Antimony Oxides*

F. SALA AND F. TRIFIRÒ

*Istituto di Chimica Industriale del Politecnico, Piazza
Leonardo da Vinci 32, 20133 Milano, Italy*

Received May 7, 1973; revised January 4, 1974

The surface and bulk chemistry of pure and mixed tin and antimony oxides prepared both by precipitation and solid state reaction have been investigated by spectroscopic and thermogravimetric techniques and by measurements of surface reactivity towards 1-butene oxidation and isomerization. Among the several Sb oxides investigated, Sb_2O_5 is the only one that presents surface oxidizing and isomerizing sites. SnO_2 shows only very little oxidizing power, attributed to the presence of free electrons due to its nonstoichiometry. The oxidizing sites of Sb_2O_5 are attributed to the presence of Sb-O double bonds and/or to surface defects. Calcination destroys the surface reactivity of pure oxides but not of the mixed ones. This particular behavior and the high surface activity of these latter oxides are attributed to their properties as controlled valence semiconductors and/or to Sb species analogous to those present in Sb_2O_5 . The oxidizing and the isomerizing sites present in mixed oxides belong to different types of surface centers. Free antimony oxides dispersed in mixed oxides exhibit a reduction rate higher than pure Sb oxides. This phenomenon is decreased by a high temperature calcination.

INTRODUCTION

The catalysts used in the selective oxidation and ammonoxidation of olefins can be divided into two classes: (1) mixed MoO_3 based oxides, such as Bi_2O_3 - MoO_3 , Fe-Te-Mo-O, Ce-Te-Mo-O (1); (2) mixed Sb_2O_4 based oxides, such as SnO_2 - Sb_2O_4 (2), UO_3 - Sb_2O_4 (3-5), Fe_2O_3 - Sb_2O_4 (6, 7).

A common and typical property of the second class of catalysts is the high activation temperature that is required to obtain high selectivity in oxidation reactions. In the case of Sn-Sb oxide based catalysts, several interpretations have been given in order to explain why a high calcination temperature is required; (i) according to Wakabayashi, Kamiya and Ohta (8) the amount of antimony dissolved in the SnO_2 lattice must be increased; (ii) according to Godin, McCain and Porter (9), microporosity must be destroyed; (iii) according to Roginskaya *et al.* (10) transformation of

Sb^{5+} to Sb^{3+} must be obtained. However, all these authors (8-10) agree that, during high temperature treatment, there is no formation of any compound, but of a solid solution of antimony oxide in SnO_2 . Discrepancies are found in the literature concerning the nature of the chemical species that are active in oxidation: (i) Wakabayashi, Kamiya and Ohta (11) stated that the active species consist of Sn^{4+} ions and that antimony labilizes the Sn-O bonds; (ii) according to Godin, McCain and Porter (9), the active sites are octahedrally coordinated Sb^{5+} ions dissolved in the SnO_2 lattice; (iii) Roginskaya *et al.* (10) stated that the activity of mixed oxides is caused by the presence of Sb^{3+} ions; (iv) Trimm and Gabbay (12) suggested that the oxidizing sites in Sn-Sb oxide must be connected with Sn^{4+} ions and that antimony oxides might somehow be involved in the allylic abstractions of hydrogen from olefins. In this work, the nature of the chemical species present in Sn-Sb oxides prepared by different methods have been investigated by

*This work was sponsored by the Consiglio Nazionale delle Ricerche, Rome, Italy.

spectroscopic analysis, and by measurements of the lability of lattice oxygen and of the activity in oxidation and isomerization of 1-butene at low temperature. For comparison pure Sn and Sb oxides were also studied.

EXPERIMENTAL METHODS

Preparation of pure and mixed oxides.

Sn-Sb oxides with a ratio Sn/Sb = 4, were prepared according to the two following methods: (i) This method involved precipitation, adding SbCl_5 to a SnCl_2 solution and neutralizing with ammonia, according to method 1 described in the Br. Pat. 876446 to Distillers Co. Such an oxide is designated Mp. The precipitate was calcined in air first at 500°C for 16 hr, then at 600 or 700 or 800 or 900°C for 1 hr and at 900°C for 3 and 15 hr. (ii) This method involved solid state reaction between finely ground SnO_2 and Sb_2O_3 , Sb_2O_4 , Sb_2O_5 , respectively. Calcination was carried out in air at 500°C for 16 hr and then at 900°C for 1 hr. These oxides are designated as Ms1, Ms2 and Ms3, respectively.

Sb oxides were prepared according to the two following methods: (i) Sb-1 was prepared and calcined in the same way as Mp (by hydrolysis of SbCl_5 in distilled water and addition of ammonia until pH 6); (ii) Sb-2 was prepared by hydrolysis of SbCl_5 in distilled water at 20°C and calcined at the same temperature as Mp. Sn oxide was prepared and calcined in the same way as Mp. All catalysts after calcination were kept in a drier with P_2O_5 . A portion of Mp was kept in a humidifier at 20°C for 4 hr before using it as a catalyst.

Materials. SbCl_5 , $\text{SnCl}_2 \cdot 2\text{H}_2\text{O}$, Sb_2O_3 and SnO_2 were RP. Carlo Erba reagents. 1-butene (99.9%) and cylinders of H_2 , He, and air supplied by SIO were used. Sb_2O_4 used in the solid state preparation of Ms2 was prepared by calcination of Sb-2 in air at 500°C for 16 hr and at 900°C for 1 hr. For the preparation of Ms3, Sb-2 calcined at 350°C for 2 hr was used.

Measurements of activity. Oxidation and isomerization of 1-butene (5% in air) were carried out at 250°C in a batch stirred tank reactor (13). Analysis of products was car-

ried out with a Carlo Erba Fractovap-C gas chromatograph, with a dimethylsulfolane on chromosorb C column 6 m long; air, CO_2 , 1-butene, *trans*-2-butene, *cis*-2-butene and butadiene were separated in that order.

Thermal balance measurements. Reduction and oxidation runs were carried out in a thermal balance Adamel TH 59-2 either with a constant increase of temperature (150°C/hr) or at a constant temperature (500°C). The gas streams used were a He-H_2 mixture (20% of H_2 by volume) for reduction runs and air for oxidation runs. In both cases a 50 liter/hr flow rate was used.

X-Ray powder data. X-Ray diffraction patterns were recorded by a Geiger counter Philips spectrogoniometer with $\text{Cu-K}\alpha$ radiation.

Infrared spectra. Infrared spectra were recorded by a Perkin-Elmer 457 spectrophotometer, using KBr discs.

Electronic spectra. Diffuse reflectance spectra of finely ground samples were recorded in the 250–700 nm range by a Cary 15 instrument having a diffuse reflectance attachment.

RESULTS

Chemical Modifications During High Temperature Treatment

Sn Oxides. No change was detected in X-ray patterns of Sn oxides during calcination from 500 to 900°C. X-Ray patterns correspond to that reported for SnO_2 (14). Also in the ir spectra of Sn oxides no change was observed during calcination (Fig. 1a and b). Figure 2 shows the diffuse reflectance spectra. Sn oxide exhibits an absorption in the 350–460 nm region (Fig. 2a and b), which decreases after calcination at 900°C (Fig. 2c). Browne, Craig and Davidson (15) have observed an absorption in the 350–460 nm region when analyzing a solution of Sn^{2+} and Sn^{4+} , and have attributed it to charge transfer transitions between the two cations. In the case of our SnO_2 , charge transfer transitions may be due to the presence of Sn^{2+} defects, which practically disappear after calcination at 900°C.

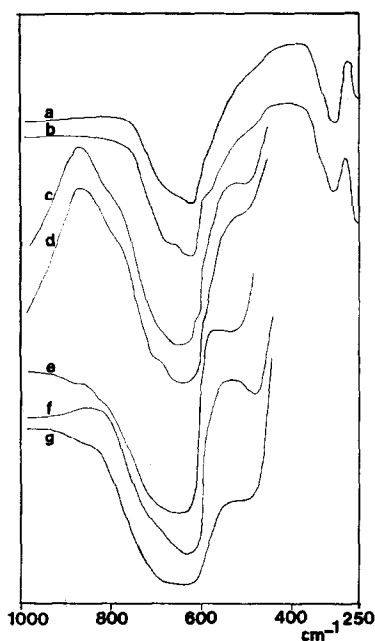


FIG. 1. Infrared spectra of Sn oxide and of mixed oxides: (a) Sn oxide, 500°C, 16 hr; (b) Sn oxide, 900°C, 1 hr; (c) Mp, 500°C, 16 hr; (d) Mp, 900°C, 1 hr; (e) Ms1, 900°C, 1 hr; (f) Ms2, 900°C, 1 hr; (g) Ms3, 900°C, 1 hr.

Sb oxides. Sb-1 calcined from 500 to 800°C is a white compound which shows the X-ray pattern of Sb_2O_5 (14). After calcination at 900°C for 1 hr, the peaks of α - Sb_2O_4 and β - Sb_2O_4 (14) were present.

After calcination at 900°C for 3 hr the intensities of the peaks of α - Sb_2O_4 were strongly decreased and after a further calcination for 12 hr only the peaks of β - Sb_2O_4 were present. Figure 3 reports the ir spectra. No change in the spectra occurs during calcination from 500 to 800°C (Fig. 3a). Spectrum modification taking place after calcination at 900°C for 1 hr (Fig. 3b) corresponds to the formation of α,β - Sb_2O_4 , in agreement with the X-ray pattern. No change in the ir spectra was observed after calcination at 900°C for a longer time. In the ir spectrum of Sb-1 calcined at 400°C, bands at 1420, 1620, 3030, 3410 cm^{-1} , which are typical of adsorbed NH_3 (16), are present. Diffuse reflectance spectra are shown in Fig. 4; no change was observed during calcination from 500 to 800°C (Fig. 4a and b). After calcination at 900°C for 1 hr and 15 hr, an absorption develops in the 400–500 nm region (Fig. 4c).

Sb-2 calcined at 500 and 600°C becomes yellow and amorphous. After calcination at 700°C, it becomes crystalline and its X-ray pattern corresponds to that of Sb_2O_5 (14) (like Sb-1). After a further calcination at 800°C, Sb-2 becomes white. In the X-ray patterns of samples calcined at 900°C for 1 hr, the ratio between the intensities of the characteristic peaks of α - Sb_2O_4 and of β - Sb_2O_4 is 1.1 for Sb-1 and 1.4 for Sb-2. The amount of α - Sb_2O_4 present in Sb-2

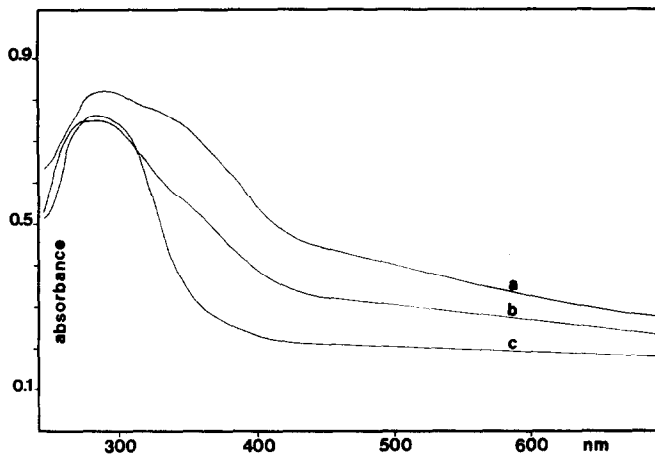


FIG. 2. Electronic spectra of pure Sn oxide: (a) Sn oxide, 500°C, 16 hr; (b) Sn oxide, 700°C, 1 hr; (c) Sn oxide, 900°C, 1 hr.

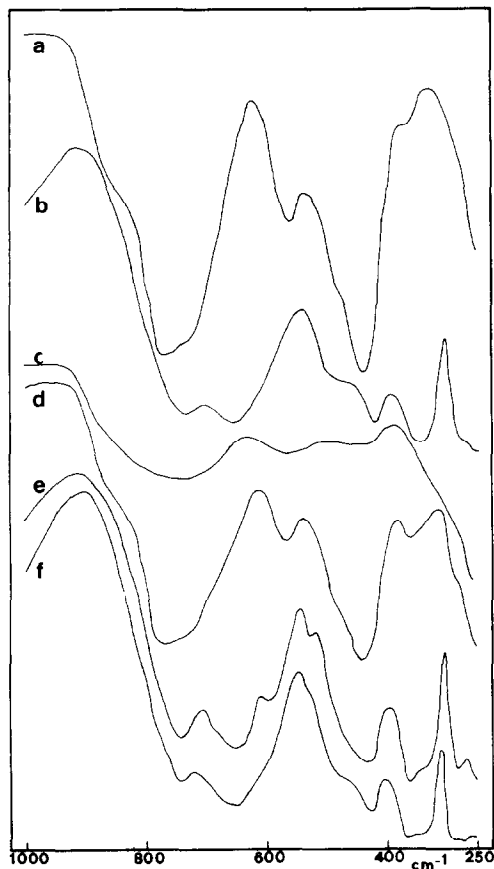


FIG. 3. Infrared spectra of pure Sb oxides: (a) Sb-1, 500°C, 16 hr; (b) Sb-1, 900°C, 1 hr; (c) Sb-2, 500°C, 16 hr; (d) Sb-2, 800°C, 1 hr; (e) Sb-2, 900°C, 1 hr; (f) Sb-2, 900°C, 15 hr.

after calcination at 900°C for 1 hr is therefore higher than in Sb-1. After a longer calcination time, the X-ray pattern of Sb-2 becomes similar to that of Sb-1 also in intensity. Figure 3 shows the ir spectra. The spectra of Sb-2 calcined at 500 and 600°C (Fig. 3c) correspond to those reported by some authors for Sb_2O_5 (17). After calcination at 800°C (Fig. 3d) the spectrum of Sb-2 becomes similar to that of Sb-1. The spectrum of Sb-2 calcined at 700°C (pale yellow) is similar to that after calcination at 800°C; however, bands are less sharp. The ir spectrum of Sb-2 calcined at 900°C for 1 hr (Fig. 3e) shows two weak bands at 610 and 525 cm^{-1} which are better resolved than in the spectrum of Sb-1 (Fig. 3b). Since Sb-2 calcined at 900°C showed a higher amount of $\alpha\text{-Sb}_2\text{O}_4$ (by X-ray analysis), we have considered these bands as being typical of $\alpha\text{-Sb}_2\text{O}_4$. After calcination at 900°C for 15 hr, these bands disappear with the formation of pure $\beta\text{-Sb}_2\text{O}_4$ (Fig. 3f). Diffuse reflectance spectra are shown in Fig. 4. A high absorption is found in the 330–500 nm region for Sb-2 calcined up to 700°C (Fig. 4d and e). After calcination of Sb-2 at 800°C or above (Fig. 4f and g) the spectra are similar to those of Sb-1.

The absorption observed in the 400–500 nm region in the diffuse reflectance spectra of α - and $\beta\text{-Sb}_2\text{O}_4$ can be attributed to charge transfer transitions between Sb^{3+}

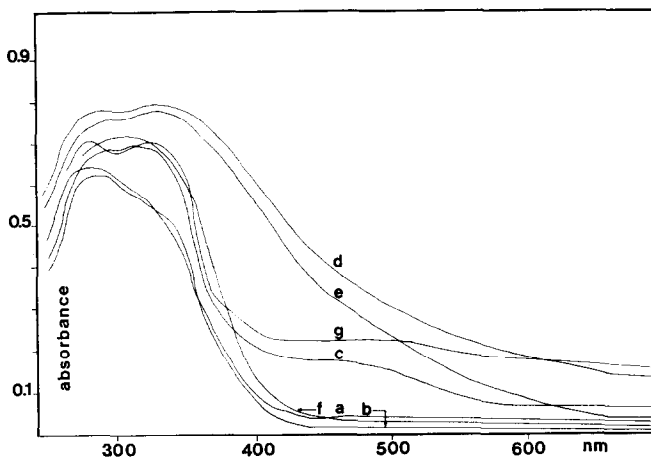


FIG. 4. Electronic spectra of pure Sb oxides: (a) Sb-1, 500°C, 16 hr; (b) Sb-1, 800°C, 1 hr; (c) Sb-1, 900°C, 1 hr; (d) Sb-2, 500°C, 16 hr; (e) Sb-2, 700°C, 1 hr; (f) Sb-2, 800°C, 1 hr; (g) Sb-2, 900°C, 1 hr.

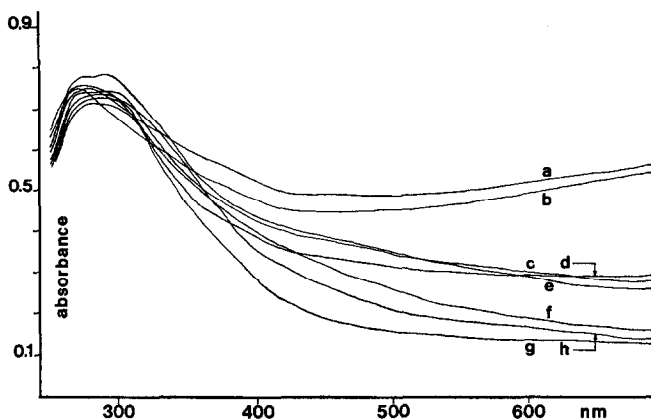


FIG. 5. Electronic spectra of mixed oxides: (a) Mp, 500°C, 16 hr; (b) Mp, 900°C, 1 hr; (c) Ms1, 900°C, 1 hr; (d) Ms2, 900°C, 1 hr; (e) Ms3, 900°C, 1 hr; (f) Ms1, 500°C, 16 hr; (g) Ms2, 500°C, 16 hr; (h) Ms3, 500°C, 16 hr.

and Sb^{5+} . Absorptions in the same region were in fact observed in a solution of Sb^{3+} and Sb^{5+} (18). As to Sb-1 calcined up to 700°C, we cannot explain the absorption in the 330–500 nm region; we consider it as characteristic of this oxide.

Sn-Sb oxides. X-Ray patterns of Sn-Sb oxides prepared by the two methods were identical with that of SnO_2 . Figure 1 shows the ir spectra. The spectra of Mp calcined from 500 to 900°C for 15 hr (Fig. 1c and d) are similar to that of SnO_2 (Fig. 1a and b); some shoulders are present, which can be attributed to free Sb oxides (no distinction is possible among Sb_2O_3 , Sb_2O_4 and Sb_2O_5). Ms oxides show bands of free Sb oxides which are more resolved (Fig. 1e, f and g)

than in Mp. Diffuse reflectance spectra are shown in Fig. 5. Mp shows an absorption in the visible region which is absent in pure oxides. No marked change in the spectra occurs during calcination from 500 to 900°C (Fig. 5a and b). The absorption in the visible region detected in mixed oxides can be attributed to charge transfer transitions between tin and antimony ions caused by the formation of a solid solution (9–11). In the case of Ms oxides, the absorption in the visible region increases during calcination from 500 to 900°C (Fig. 5c–h). Therefore we can assume that in Ms oxides during calcination at high temperature, the amount of antimony oxide dissolved in the SnO_2 lattice increases.

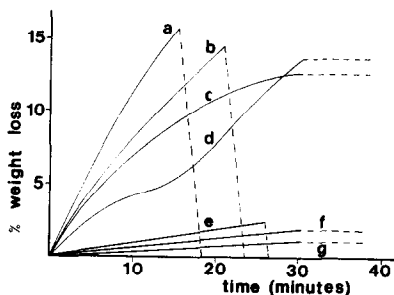


FIG. 6. Reduction and oxidation rates of pure and mixed oxides: (a) Mp, 900°C, 15 hr; (b) Ms1,2,3, 900°C, 1 hr; (c) Sb-1, 500°C, 16 hr; (d) Sb-2, 500°C, 16 hr; (e) SnO_2 , 900°C, 1 hr; (f) Sb-1, 900°C, 1 hr; (g) Sb-1, 900°C, 15 hr.

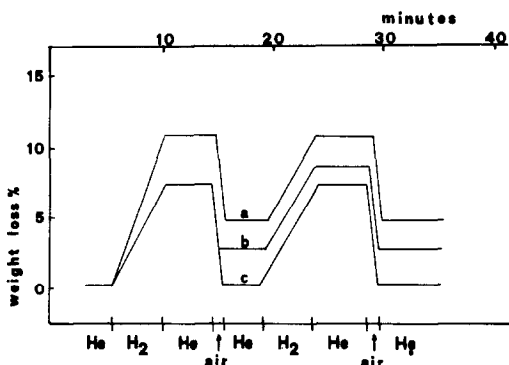


FIG. 7. Reduction and reoxidation runs of mixed oxides: (a) Mp, 500°C, 16 hr; (b) Mp, 900°C, 1 hr; (c) Mp, 900°C, 15 hr.

Redox Process

The data of reduction and oxidation runs carried out at 500°C with pure and mixed oxides are shown in Figs. 6 and 7. By spectroscopic analysis, reduction of Sb oxides was found to take place through formation of Sb_2O_4 , cubic Sb_2O_3 and then metallic Sb, while reduction of Sn oxide occurred through formation of SnO and then metallic Sn. An irreversible reduction was observed in redox processes carried out with pure Sb oxides (irrespective of their temperature of calcination and method of preparation) (Fig. 6c, d, f and g). No irreversibility was observed in reduction and reoxidation of SnO_2 (Fig. 6e). Mp and Ms oxides show high rates of reduction (Fig. 6a and b), similar to Sb_2O_5 (Fig. 6c and d), and also a high rate of oxidation similar to reduced SnO_2 (Fig. 6g). Mp provided only a partial irreversibility which was strongly reduced by calcination at 900°C for a longer time (Fig. 7). The partially irreversible reduction shown by Mp is attributed by us to the reduction of free Sb oxide present in it. The low irreversibility of Mp calcined at 900°C for 3 hr or even for longer times is attributed to the transformation of free Sb_2O_5 or $\alpha\text{-Sb}_2\text{O}_4$ into $\beta\text{-Sb}_2\text{O}_4$ (see Fig. 3b). In fact, $\beta\text{-Sb}_2\text{O}_4$ shows a very low reduction rate, as shown in Fig. 6.

Strength of Me-O Bonds

The temperatures (T_{or}) at which bulk reduction of samples calcined at different temperatures starts, are shown in Fig. 8. The T_{or} can be taken as a measure of Me-O bond strength and therefore is a parameter characterizing the surface chemistry of oxides. As to the Sn and Mp oxides, no variation of T_{or} was observed during calcination from 500 to 900°C. As to Sb oxides, differences are observed between Sb-1 and Sb-2. Sb-2 calcined at 500°C shows a T_{or} lower than Sb-1 calcined either at 500 and at 800°C. The T_{or} of Sb-2 reaches the value shown by Sb-1 only after calcination at high temperatures.

Surface Reactivity

In order to obtain information on the surface reactivity of pure and mixed oxides, we have chosen to measure the activity in 1-butene oxidation at low temperatures in a batch reactor. We have chosen these reaction conditions for the following reasons:

- i. Sb oxides deactivate very easily and therefore in a flow reactor we could not obtain information on initial activity (19);
- ii. At low temperatures, mixed oxides show not only oxidizing power towards 1-butene but also high isomerizing power (13); hence information on their acid-base properties may be also obtained.

Figures 9 and 10, respectively, show the amount of butadiene and 2-butenes versus the time of reaction of some of the investigated catalysts. From Fig. 9e and f, it is possible to observe that Sb-2 oxide deactivates after 30 min. This deactivation shown in butadiene formation is not so marked in the isomerization to 2-butenes (Fig. 10e and f). The deactivation is not observed in mixed oxides nor in SnO_2 (see Figs. 9 and 10). In Figs. 11, 12 and 13, we have summarized the results for all the oxides investigated. As a measure of the oxidizing and isomerizing power we have respectively chosen the amount of butadiene, 2-butenes and CO_2 formed after 1 hr. Oxides which give no product after 5 hr were considered inactive. Sb-1 was inactive for both reactions whatever the calcination temperature.

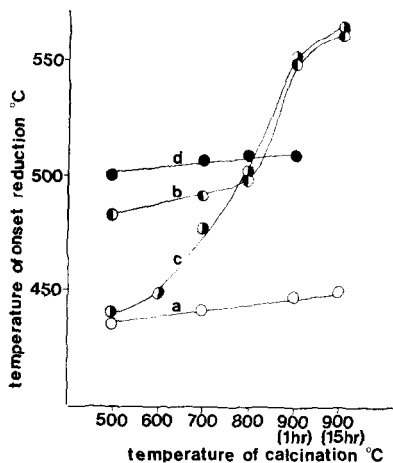


Fig. 8. Temperature of onset of bulk reduction for pure and mixed oxides: (a) Mp; (b) Sb-1; (c) Sb-2; (d) Sn.

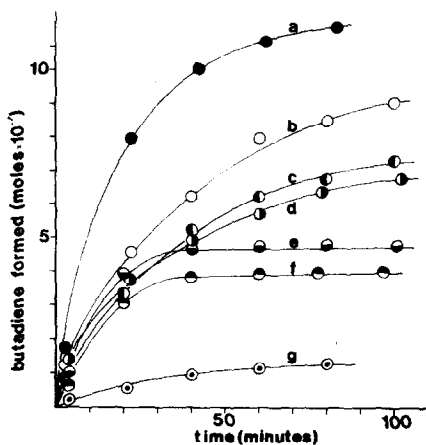


Fig. 9. Butadiene formation vs contact time for pure and mixed oxides: (a) Mp, 500°C, 16 hr; (b) Mp, 900°C, 1 hr; (c) Ms3, 900°C, 1 hr; (d) Ms1, 900°C, 1 hr; (e) Sb-2, 600°C, 1 hr; (f) Sb-2, 500°C, 16 hr; (g) Sn, 600°C, 1 hr.

Sb-2 calcined at 500°C showed high isomerizing and oxidizing power, which was destroyed during calcination at 800°C (Figs. 11b and 12b). Sb₂O₃ was found to be inactive. Sn oxide presents a low activity both in oxidation and isomerization; however, its activity markedly decreases in both reactions during calcination at high temperatures (Figs. 11c, 12c and 13c). Mp oxide is active both in oxidation and iso-

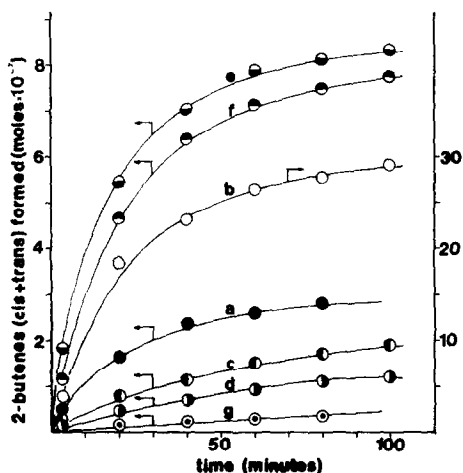


Fig. 10. 2-Butenes (*cis* + *trans*) formation vs contact time for pure and mixed oxides: (a) Mp, 500°C, 16 hr; (b) Mp, 900°C, 1 hr; (c) Ms3, 900°C, 1 hr; (d) Ms1, 900°C, 1 hr; (e) Sb-2, 600°C, 1 hr; (f) Sb-2, 500°C, 16 hr; (g) Sn, 600°C, 1 hr.

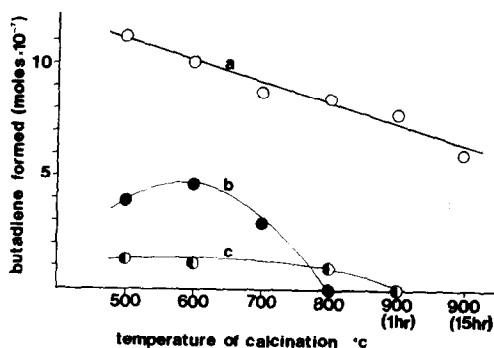


Fig. 11. Butadiene formation for pure and mixed oxides: (a) Mp, (b) Sb-2, (c) Sn. Experimental conditions: $T = 250^{\circ}\text{C}$; 1-Butene in air = 5%; catalyst = 1 g; contact time = 1 hr.

merization; during calcination at high temperature its oxidizing power decreases slowly (Fig. 11a), whereas its isomerizing power shows a sharp increase (Fig. 12a) after calcination at 900°C.

Table 1 reports the amount of butadiene, 2-butenes and CO₂, formed after 1 hr by Ms oxides calcined at 500°C for 16 hr and at 900°C for 1 hr. After calcination at 500°C the activity of Ms oxides both in oxidation and isomerization is low. Activity rises on increasing the calcination temperature. After treatment at 900°C, the oxidizing power of Ms becomes like that of Mp. On the other hand, isomerizing power is lower even at this calcination temperature. For comparison, the data obtained for Mp

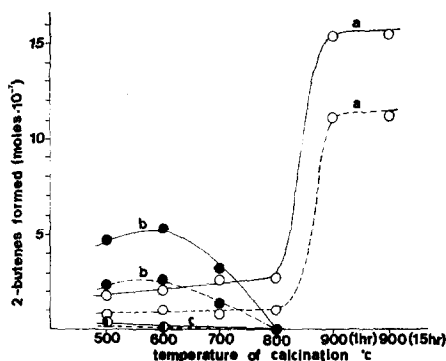


Fig. 12. 2-Butenes formation for pure and mixed oxides: (a) Mp, (b) Sb-2, (c) Sn; (—) *cis*-2-butene; (---) *trans*-2-butene. Experimental conditions as those of Fig. 11.

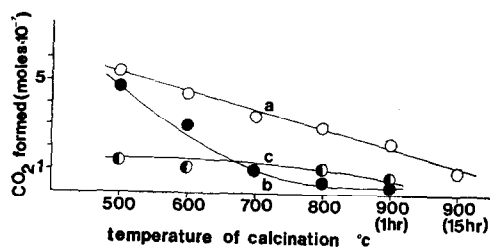


FIG. 13. Carbon dioxide formation for pure and mixed oxides: (a) Mp, (b) Sb-2, (c) Sn. Experimental conditions as those of Fig. 11.

and for Mp_{ro} (reduced and reoxidized with H_2 and air at $500^\circ C$ in the thermal balance) and for Mp oxides kept in the humidifier are also reported. Mp_{ro} calcined at $900^\circ C$ for 1 and 15 hr showed a slightly lower oxidizing power than Mp, but its isomerizing power was practically nil. The activity in isomerization of Mp kept in the humidifier is practically destroyed, while the oxidizing power is merely decreased. The activity of Ms1 calcined at $900^\circ C$ for 1 hr, washed with boiling water for 15 min and calcined

again at $900^\circ C$ for 1 hr, is also reported. After this treatment Ms1 increases its isomerizing power to a value about 5 times higher than that previously presented. The *cis/trans* ratios of the formed 2-butenes are also reported in Table 1 for all the oxides.

DISCUSSION

Surface Reactivity of Pure Oxides

As may be deduced from Figs. 11 and 12, both SnO_2 and Sb_2O_5 are active in the oxidation and isomerization of 1-butene at $250^\circ C$. The isomerizing power of SnO_2 is very low; however, it is known that this oxide, either when reduced (13) or at low reaction temperatures (20), shows a high isomerizing power. Therefore, it is rather difficult to attribute the low temperature activity presented by the mixed oxides to the active sites tied to only one of the two ions. The main difference between pure and mixed oxides is the effect of the calcination temperature on surface reactivity. In pure

TABLE I
SURFACE REACTIVITY OF MIXED OXIDES^a

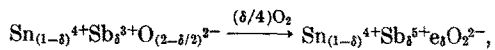
Catalyst	Butadiene formed (moles $\times 10^{-7}$)	2-Butene (<i>cis</i> + <i>trans</i>) formed (moles $\times 10^{-7}$)	CO ₂ formed (moles $\times 10^{-7}$)	<i>cis/trans</i> ratio of formed 2-butenes
Mp calcined at $500^\circ C$, 16 hr	11.1	2.6	4.08	2.6
900°C, 1 hr	7.95	26.65	2.25	1.4
Mp calcined at $500^\circ C$, 16 hr, then 4 hr in humidifier at $20^\circ C$	7.45	0.90	4.55	2
Mp calcined at $900^\circ C$, 1 hr, then 4 hr in humidifier at $20^\circ C$	5.95	0.96	2.36	2
Mp_{ro} calcined at $900^\circ C$, 1 hr	5.01	1.23	1.07	2
15 hr	4.6	1.01	0.96	2
Ms1 calcined at $500^\circ C$, 16 hr	1.14	1.15	0.39	2
Ms2 calcined at $500^\circ C$, 16 hr	1.1	1.06	0.35	2
Ms3 calcined at $500^\circ C$, 16 hr	2.04	1.14	0.41	2
Ms1 calcined at $900^\circ C$, 1 hr	5.76	0.94	1.38	2.7
Ms2 calcined at $900^\circ C$, 1 hr	4.88	0.86	0.63	2.7
Ms3 calcined at $900^\circ C$, 1 hr	6.23	1.51	0.95	2.7
Ms1 calcined at $900^\circ C$, 1 hr, boiled in H_2O for 15 min, then calcined at $900^\circ C$, 1 hr	4.58	4.64	0.54	2
Ms1 calcined at $800^\circ C$, 1 hr	1.82	1.20	0.50	2

^a Experimental conditions: $T = 250^\circ C$; 1-butene initial: 5% in air; catalyst: 1 g; contact time: 1 hr.

oxides the calcination at high temperature destroys the surface reactivity, but the opposite is true for the mixed oxides. (Figs. 11 and 12 and Table 1). For SnO_2 the surface reactivity disappears with decreasing absorption in the visible (Fig. 2), absorption which, like the semiconductivity of SnO_2 (21-24), is attributed to nonstoichiometry. The role of free electrons and nonstoichiometry determining the surface reactivity of oxides was proposed by many authors (25, 26). Also in the case of Sb_2O_5 the surface reactivity occurs when an absorption in the visible is present (Figs. 4, 11b and 12b). In fact Sb-1 is inactive, and Sb-2 becomes inactive at 800°C (Figs. 11b and 12b) when it turns from yellow to white color. Other differences between yellow and white Sb_2O_5 are that the former is amorphous with a T_{or} of 450°C (Fig. 8c) while the latter is crystalline with a higher T_{or} (485°C). The structure of Sb_2O_5 is unknown; however, from Mössbauer spectra, it was deduced that it has an octahedral coordination of antimony (27). The ir spectrum of white Sb_2O_5 suggests the presence of $\text{Sb}=\text{O}$ double bonds, absorption at 820 cm^{-1} (Fig. 3) being typical of $\text{Sb}=\text{O}$ bonds in antimonyl compounds (28, 29). Infrared bands of Sb-2 are too large to be interpreted (Fig. 3c). The visible absorption cannot be clearly explained, but may be due to electronic defects. The presence of $\text{Sb}=\text{O}$ in Sb_2O_5 shows analogy with active molybdates, which are well-known selective oxidation catalysts and where $\text{Mo}=\text{O}$ bonds have been postulated as the active sites in the oxidative dehydrogenation of olefins (30). However, we cannot say whether $\text{Sb}=\text{O}$ bonds and/or a particular electronic defect are responsible for the activity of Sb_2O_5 . White Sb_2O_5 , which has $\text{Sb}=\text{O}$ bonds, is inactive. However, this can be explained by assuming reduction during calcination, due very probably to NH_3 adsorbed in the precipitation. This NH_3 , released during calcination, can produce surface reduction even at relatively low temperatures (about 500°C). This fact can also explain the high T_{or} and the absence of absorption in the electronic spectra.

Nature of the Oxidizing Sites in Mixed Oxides

Sb^{3+} , introduced as a dopant in SnO_2 , produces a donor level which is ionized already at room temperature (23, 24), and hence a marked increase of conductivity results (9, 24, 31). Thus there are more free electrons at 250°C in the solid solution than in nonstoichiometric SnO_2 . According to Vincent (32), Sb-doped SnO_2 is a *controlled valence semiconductor* (33), which means that introducing Sb^{3+} ions produces no other defects, in contrast to *nonstoichiometric semiconductors*. The conductivity is due to the electrons formed by oxidation in air at high temperature, according to the reaction (32):



where δ is the amount of antimony in the solid solution. The absence of free electrons in anionic vacancies in Sb-doped SnO_2 explains the three following phenomena: (i) the stability of its semiconductivity and surface reactivity during calcination in air at high temperature (oxidation destroys semiconductivity in a nonstoichiometric *n*-type oxide but develops it in the case of a controlled valence semiconductor (1)); (ii) the absence of radicals $\text{O}_{2\text{ads}}$ found on reduced pure SnO_2 following oxygen adsorption and electron trapping (34, 35); (iii) the formation of a solid solution accompanied by the stabilization of Sb^{5+} ions in octahedral coordination, which according to Godin, McCain and Porter (9) are the active oxidizing sites. The mixed oxides and the yellow Sb-2, which is the only antimony oxide active in the dehydrogenation of 1-butene (Fig. 11b), have the same T_{or} values (Fig. 8a and c) and similar reduction rates (Fig. 6a, b and d). $\text{Sb}=\text{O}$ groups, observed in Sb_2O_5 , cannot be present in the bulk of the mixed oxides owing to the high symmetry of the rutile structure of doped SnO_2 ; however, their presence is possible at the surface. Thus, solution of Sb in SnO_2 leads to: (i) increase in the quantity and in the stability towards high temperatures of free electrons; (ii) stabilization towards calcination and the redox process

of Sb^{5+} ions, similar in type to that present in Sb_2O_5 . The activity shown by the mixed oxides can be attributed to both these factors or to only one of them.

Nature of the Acidic Sites in Mixed Oxides

No correlation exists between oxidizing and isomerizing power of mixed oxides. In fact, as shown in Table 1, either the pre-humidification of the catalyst or a redox cycle destroys the isomerizing power, but not the oxidizing one. Furthermore, the mixed oxides prepared by different ways present the same oxidizing power but different isomerizing activity (Table 1). The strong increase of isomerizing power presented by Mp when calcined at 900°C (Fig. 12a) and the inhibiting effect of water implies that the surface isomerizing sites are Lewis-type acidic centers formed by surface dehydration. In fact, after washing Ms1 with water and calcining at 900°C , the isomerizing power increases (Table 1). Some hydroxylated oxides, such as $\text{Sb}_3\text{O}_6(\text{OH})$ (36) and $\text{H}_2\text{Sb}_2\text{O}_5(\text{OH})_2$ (37), are formed during high temperature treatments of hydrated Sb_2O_5 . We may suppose that these species are present on the surface of the mixed oxides. The hypothesis of some migration of Sb in SnO_2 at 900°C , making Sb-OH ions near one another, permits dehydration. The strong increase of SnO_2 doping by Sb at 900°C observed for Ms1,

Ms2, Ms3 (Fig. 5c-h and Table 1) justifies the possibility of a rearrangement and/or of a migration of Sb ions at this temperature.

The Role of the Calcination Temperature

The high calcination temperature produces three different effects on mixed oxides: (i) for Ms, a sharp increase in the SnO_2 doping by antimony revealed both by the increase of absorption in the visible and by the amount of butadiene formed; (ii) for Mp, a sharp increase of the isomerizing power which we have attributed to a migration of Sb^{5+} ions in the SnO_2 lattice and to a subsequent surface dehydration; (iii) the disappearing of the irreversible weight loss in the redox cycle for Mp (Fig. 7). Since only 7% of Sb can dissolve in SnO_2 (9), in our catalysts there is 13% of free antimony oxide, to whose irreversible reduction (Fig. 6c, d, f and g) the weight loss may be attributed. However, Table 2 shows that Mp gives irreversible reductions, sometimes corresponding to the reduction of almost all the Sb oxide to metallic antimony. Since only the free antimony oxide (13%) can be reduced irreversibly, a further phenomenon must exist, for example a partial sublimation of the formed metallic Sb. Decrease of the irreversible weight loss on increasing the temperature and duration of calcination

TABLE 2
WEIGHT LOSSES OF PURE AND MIXED OXIDES DURING REDUCTION

Reduction		Calcd wt loss (%)	Sample	Observed wt loss (%) ^a
From	To			
Sb_2O_5	Sb_2O_4	4.45	Sb-1 500°C 16 hr (Sb_2O_5)	4.05
Sb_2O_5	Sb_2O_3	9.9	Sb-2 500°C 16 hr (Sb_2O_5)	2.57
Sb_2O_5	Sb	24.7	α, β - Sb_2O_4	0.44
* Sb_2O_4	Sb_2O_3	5.2	β - Sb_2O_4	0.24
Sb_2O_4	Sb	20.8	Mp 500°C 16 hr	21.6 ^b
			Mp 900°C 1 hr	12.9 ^b
			Mp 900°C 15 hr	~0

^a Observed after 5 min of reduction.

^b Irreversible weight loss (%) for Mp (20% of Sb present) $\times 5$ (to report data to 100% Sb oxide, to make possible comparisons). For simplification, all the antimony present (20%) has been taken into account for this calculation; but, since very probably only 13% is free and subsequently reducible, the phenomenon would be even more considerable quantitatively.

can be explained by the transformation of free antimony oxide from Sb_2O_5 (present at 500°C) into $\alpha,\beta\text{-Sb}_2\text{O}_4$ (present at 900°C for 1 hr) and $\beta\text{-Sb}_2\text{O}_4$ (present at 900°C for 15 hr), which feature much lower reduction rates (Fig. 6f and g). Table 2 shows that the reduction rate (irreversible weight loss after 5 min of reduction) of free antimony oxides present in Mp is higher than that of pure Sb oxides. Only after calcination at 900°C for 15 hr are the reduction rates the same. Therefore, the free Sb oxide presents a higher reactivity that can be due to a doping by tin or to a high surface area.

ACKNOWLEDGMENT

We gratefully thank Professor I. Pasquon for his interest and for encouraging this work.

REFERENCES

1. VOGEL, H. H., AND ADAMS, C. H., in "Advances in Catalysis" (D. D. Eley, H. Pines and P. B. Weisz, Eds.), Vol. 17, p. 131. Academic Press, New York, 1967.
2. Distillers, *Brit. Pat.* 864666; 876446; 904602; 1007685.
3. SOHIO, *U. S. Pat.* 3198750; 3308151.
4. GRASELLI, R. K., AND SURESH, D. D., *J. Catal.* **25**, 273 (1972).
5. SIMONS, T. G. J., HOUTMAN, P. N., AND SCHUIT, G. C. A., *J. Catal.* **23**, 110 (1971).
6. U. C. B., *Belg. Pat.* 622025; 633451 and *Neth. Pat.* 6602866.
7. SOHIO, *U. S. Pat.* 3338952; 3445521 and *Ger. Offen.* 1265731.
8. WAKABAYASHI, K., KAMIYA, Y., AND OHTA, N., *Bull. Chem. Soc. Jap.* **40**, 2172 (1967).
9. GODIN, G. W., MCCAIN, C. C., AND PORTER, E. A., *Proc. Int. Congr. Catal., 4th (1968)* **1**, 271, (1971).
10. ROGINSKAYA, Y. E., DULIN, D. A., STROEVA, S. S., KULKOVA, N. V., AND GEL'BSHTEIN, A. J., *Kinet. Katal.* **9**, 1143 (1968).
11. WAKABAYASHI, K., KAMIYA, Y., AND OHTA, N., *Bull. Chem. Soc. Jap.* **41**, 2776 (1968).
12. TRIMM, D. L., AND GABBAY, D. S., *Trans. Faraday Soc.* **67**, 2782 (1971).
13. TRIFIRÒ, F., VILLA, P. L., AND PASQUON, I., *Chim. Ind. (Milan)* **52**, 857 (1970).
14. SMITH, J. V. (Ed.), "Inorganic Index to the Powder Diffraction File." ASTM, Philadelphia, 1967.
15. BROWNE, C. I., CRAIG, R. P., AND DAVIDSON, N., *J. Amer. Chem. Soc.* **73**, 1946 (1951).
16. BADILA, M. R., AND KANTNER, T. R., *J. Phys. Chem.* **71**, 467 (1967).
17. MILLER, F. A., AND WILKINS, C. H., *Anal. Chem.* **24**, 1275 (1952).
18. DAY, P., *Inorg. Chem.* **2**, 452 (1963).
19. SALA, F., thesis, Univ. of Milan, 1971.
20. KEMBALL, C., LEACH, H. F., AND SHANNON, I. R., *J. Catal.* **29**, 99 (1973).
21. MARLEY, J. A., AND DOCKERTY, R. C., *Phys. Rev. A* **140**, 304 (1965).
22. NAGASAWA, M., SHIONOYA, S., AND MAKISHIMA, S., *Jap. J. Appl. Phys.* **4**, 165 (1965).
23. NAGASAWA, M., AND SHIONOYA, S., *Jap. J. Appl. Phys.* **10**, 472 (1971).
24. LEJA, E., *Acta Phys. Pol. A* **38**, 165 (1970).
25. WOLKENSTEIN, T., in "Advances in Catalysis" (D. D. Eley, P. W. Selwood and P. B. Weisz, Eds.), Vol. 12, p. 189. Academic Press, 1960.
26. STONE, F. S., in "Advances in Catalysis" (D. D. Eley, P. W. Selwood and P. B. Weisz, Eds.), Vol. 13, p. 1. Academic Press, New York, 1962.
27. LONG, G. G., STEVENS, J. G., AND BOWEN, L. H., *Inorg. Nucl. Chem. Lett.* **5**, 799 (1969).
28. DEKNICKE, K., *Chem. Ber.* **97**, 3358 (1964).
29. DEHNICKE, K., AND WEIDLEIN, J., *Z. Anorg. Allg. Chem.* **342**, 225 (1966).
30. TRIFIRÒ, F., AND PASQUON, I., *J. Catal.* **12**, 412 (1968).
31. AITCHISON, R. E., *Aust. J. Appl. Sci.* **5**, 10 (1954).
32. VINCENT, C. A., *J. Electrochem. Soc.* **113**, 515 (1972).
33. VERWEY, E. J. W., in "Semiconducting Materials" (H. K. Henisch, Ed.), Butterworth, London (1951).
34. VAN HOOFF, J. H. C., AND VAN HELDEN, J. F., *J. Catal.* **8**, 199 (1967).
35. SIMONS, T. G. J., VERHEIJEN, E. J. M., PATIST, P. A., AND SCHUIT, G. C. A., *Advan. Chem. Ser.* **76**, 261 (1968).
36. DIHLSTRÖM, K., AND WESTGREN, A., *Z. Anorg. Allg. Chem.* **235**, 153 (1937).
37. ABE, M., AND ITO, T., *Bull. Chem. Soc. Jap.* **41**, 2366 (1963).